

## Surface properties and photocatalytic activity of nanocrystalline titania films

<strong/>

Simonsen, Morten Enggrob; Jensen, Henrik; Li, Zheshen; Søgaard, Erik Gydesen

*Published in:*

Journal of Photochemistry and Photobiology, A: Chemistry

*DOI (link to publication from Publisher):*

[10.1016/j.jphotochem.2008.07.013](https://doi.org/10.1016/j.jphotochem.2008.07.013)

*Publication date:*

2008

*Document Version*

Accepted author manuscript, peer reviewed version

[Link to publication from Aalborg University](#)

*Citation for published version (APA):*

Simonsen, M. E., Jensen, H., Li, Z., & Søgaard, E. G. (2008). Surface properties and photocatalytic activity of nanocrystalline titania films: . *Journal of Photochemistry and Photobiology, A: Chemistry*, 200(2-3), 192-200. <https://doi.org/10.1016/j.jphotochem.2008.07.013>

### General rights

Copyright and moral rights for the publications made accessible in the public portal are retained by the authors and/or other copyright owners and it is a condition of accessing publications that users recognise and abide by the legal requirements associated with these rights.

- Users may download and print one copy of any publication from the public portal for the purpose of private study or research.
- You may not further distribute the material or use it for any profit-making activity or commercial gain
- You may freely distribute the URL identifying the publication in the public portal -

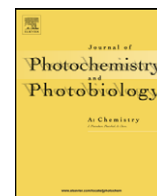
### Take down policy

If you believe that this document breaches copyright please contact us at [vbn@aub.aau.dk](mailto:vbn@aub.aau.dk) providing details, and we will remove access to the work immediately and investigate your claim.



Contents lists available at ScienceDirect

# Journal of Photochemistry and Photobiology A: Chemistry

journal homepage: [www.elsevier.com/locate/jphotochem](http://www.elsevier.com/locate/jphotochem)

## Surface properties and photocatalytic activity of nanocrystalline titania films

Morten E. Simonsen<sup>a</sup>, Henrik Jensen<sup>c</sup>, Zheshen Li<sup>b</sup>, Erik G. Søgaard<sup>a,\*</sup><sup>a</sup> Aalborg University, Department of Chemical Engineering, Niels Bohrs vej 8, 6700 Esbjerg, Denmark<sup>b</sup> University of Aarhus, Institute for the Storage Ring Facilities, 8000 Aarhus C, Denmark<sup>c</sup> SCF-Technologies A/S, Smedeholm 13B, 2730 Herlev, Denmark

### ARTICLE INFO

#### Article history:

Received 1 April 2008

Received in revised form 2 July 2008

Accepted 15 July 2008

Available online 3 August 2008

#### Keywords:

TiO<sub>2</sub> films

Photocatalysis

XPS

Hydroxyl radicals

AFM

### ABSTRACT

In this work the efficiency and physicochemical details of a thin film produced by help of a microwave assisted sol gel technique is compared to different commercial powders (Degussa P25 and Hombikat UV100) deposited on glass substrates. Furthermore, a supercritical produced TiO<sub>2</sub> powder (SC 134) was included in the comparison.

The prepared TiO<sub>2</sub> films were characterized using XRD, XPS, AFM, DSC and DLS. The photocatalytic activity was determined using stearic acid as a model compound. Investigation of the prepared films showed that the Degussa P25 film and the sol–gel film were the most photocatalytic active films. The activity of the films was found to be related to the crystallinity of the TiO<sub>2</sub> film and the amount of surface area and surface hydroxyl groups. Based on the XPS investigation of the films before and after UV irradiation it was suggested that the photocatalytic destruction of organic matter on TiO<sub>2</sub> films proceeds partly through formation of hydroxyl radicals which are formed from surface hydroxyl groups created by interactions between adsorbed water and vacancies on the TiO<sub>2</sub> surface. Furthermore a correlation between the amount of OH groups on the surface of the different TiO<sub>2</sub> films and the photocatalytic activity was found.

© 2008 Elsevier B.V. All rights reserved.

### 1. Introduction

Heterogeneous photocatalysis is one of the advanced oxidation processes that couples low-energy ultraviolet light with semiconductors acting as photocatalysts. In this process completely mineralization of the organic pollutants to carbon dioxide and mineral acids is achieved [1,2]. TiO<sub>2</sub> is the most often used semiconductor in photocatalysis due to high activity, chemical stability, and it is not subject to photocorrosion [2].

The photocatalytic activity of TiO<sub>2</sub> has been found to be tied to the surface properties of the catalyst. Among others Jensen et al. investigated the influence of the preparation method on the photocatalytic activity of TiO<sub>2</sub> powders [3]. Some of the particle properties which are known to affect the photocatalytic activity are particle size, crystal structure, absolute crystallinity, amounts and the identity of defects, incident light intensity, adsorption of pollutants, pH of the solution, and preparation method [4–7].

In the field of photocatalysis, most applications are concerned with water and air purification or self-cleaning properties of different materials. Considerable amount of work has been done on TiO<sub>2</sub>-modified materials for self-cleaning windows and building

surfaces [7,8]. In the case of self-cleaning applications, TiO<sub>2</sub> is deposited on the substrate as a thin film. The basic idea is that the surface can be kept clean by the action of sunlight and rainwater, due to the photocatalytic and superhydrophilic properties of TiO<sub>2</sub> [9].

Early work on water purification using photocatalysis mainly focused on the photomineralization of organics dissolved in aqueous solution usually employing the semiconductor in the form of a powder suspension. The use of TiO<sub>2</sub> in suspension is efficient due to the large surface area of the catalyst and the absence of mass transfer limitations [2,10]. However, the use of suspensions requires an additional separation step which is both time consuming and expensive [2,10,11]. In order to overcome these obstacles immobilization of the TiO<sub>2</sub> catalyst in the photoreactor seems to be an important step of improvement.

Considerable amount of research has been done on immobilization of TiO<sub>2</sub> for both self-cleaning and purification purposes. Different preparation methods for the immobilization of TiO<sub>2</sub> on substrates have been investigated including organic precursor decomposition, chemical vapor deposition (CVD), screen printing techniques, and sol–gel methods [12].

In this work we want to compare the efficiency and physicochemical details of a thin film produced by help of a microwave assisted sol gel technique with different commercial powders all deposited on glass substrates. The commercial powders were two

\* Corresponding author. Tel.: +45 99407622; fax: +45 75453643.  
E-mail address: [egs@aaue.dk](mailto:egs@aaue.dk) (E.G. Søgaard).

of the most widely used powders in photocatalytic degradation of organic pollutants in aqueous solution. Furthermore, a supercritical produced TiO<sub>2</sub> powder prepared in our laboratory (SC 134) was included in the comparison. The TiO<sub>2</sub> powder produced in supercritical CO<sub>2</sub> has a small primary particle size and a narrow particle size distribution [13].

The work presented in this article shows that the physical and chemical properties of the prepared TiO<sub>2</sub> films are closely related to the photocatalytic activity of the films. In order to optimize the activity it is important to have precise knowledge of the properties of the prepared film all the way from preparation of the powder or sol–gel paste through dispersion of the particles to immobilization of the particles on a substrate. To obtain the detailed knowledge on similarities and differences of the photocatalytic films the films were characterized by X-ray diffraction (XRD), atomic force microscopy (AFM), dynamic light scattering (DLS), and differential scanning calorimetry (DSC). Furthermore, the surface properties of the TiO<sub>2</sub> films were examined by help of X-ray photoelectron spectroscopy (XPS) before and after UV irradiation. The idea was to reveal surface changes occurring as a result of the photocatalytic activation of the films and to be able to discuss a physicochemical model of these changes based on the experimental results. The photocatalytic activity of the films was determined using stearic acid as a model compound.

## 2. Materials and methods

### 2.1. Preparation of TiO<sub>2</sub> films

#### 2.1.1. Preparation of TiO<sub>2</sub> films from titania powders

Titania films were prepared from the three different powders. For the preparation of the films two commercially available TiO<sub>2</sub> powders (Degussa P25 and Hombikat UV100) and one TiO<sub>2</sub> powder produced in our laboratories in supercritical CO<sub>2</sub> (SC 134) were used. The preparation methods of the powders are described by Jensen et al. [3,14]. The films were prepared by suspending the TiO<sub>2</sub> powder in a 95/5% (w/w) methanol/water mixture which was sonicated for 1 h. In order to obtain films of different photocatalytic activity the amount of TiO<sub>2</sub> powder added to the methanol/water solution varied between 0.5 and 10% (w/w).

The pH of the suspension was adjusted at pH 3 using HNO<sub>3</sub> to obtain better adhesion between the TiO<sub>2</sub> and the glass substrate (microscope slide). The pH of the suspension was below the isoelectric point of TiO<sub>2</sub> (reported values 5.6–6.2) resulting in TiO<sub>2</sub> having a positive charge. Reported values of the isoelectric point of SiO<sub>2</sub> range from 1.85 to 2.7 resulting in the glass substrate having a negative charge at pH 3. Therefore, it is expected that there is an electrostatic attraction between the two surfaces that will enhance the adhesion [11,15].

The nanocrystalline films were immobilized on a microscope slide by applying the doctor blade method described by Mills et al. [16]. The dried films were placed in a furnace at 450 °C for 1 h to secure adhesion between the TiO<sub>2</sub> film and the glass.

#### 2.1.2. Preparation of nanocrystalline sol–gel titania films

The sol–gel TiO<sub>2</sub> film was prepared from a modified sol–gel method initially described by Mills et al. and Barbé et al. [16,17]. The sol–gel method produces a TiO<sub>2</sub> paste which can be coated onto different substrates. The TiO<sub>2</sub> paste was prepared by adding 5 ml titanium (IV) tetraisopropoxide to 1.1 ml glacial acetic acid which was mixed with 30 ml 0.1 M nitric acid solution. The solution was placed in a microwave reactor (Anton Paar, Multiwave 3000) in order to control the sol–gel synthesis. A temperature ramp of 100 min was used to reach the final temperature of 220 °C and a

pressure of 60 bar. The final conditions were held for 100 min before allowing the system to cool down. The solution in the microwave reactor was stirred at 400 rpm during the entire process. After synthesis the particles were redispersed using ultra sound. The solution was rotary evaporated until the TiO<sub>2</sub> content was 10 wt%. The pH of the final TiO<sub>2</sub> paste was approximately 3 as in the case of the deposition of the different titania powders.

The films were prepared by applying the doctor blade technique described in [16]. After drying for 30 min the films were placed in a furnace at 450 °C for 1 h to obtain a better adhesion of the film to the glass.

#### 2.1.3. Preparation of powder samples

Apart from the film, also powder samples were prepared in order to determine their physical and chemical properties. Suspensions of TiO<sub>2</sub> powder with the same compositions used to prepare the films were dried at 105 °C in air. In addition the sol–gel paste was dried at 105 °C in order to obtain a powder. The four powder samples were then heat treated for 1 h at 450 °C and grounded in an agate mortar.

### 2.2. XRD analysis

In the present work reflection X-ray diffraction (XRD) was used to determine the presence of anatase and rutile phases in the TiO<sub>2</sub> films. The XRD spectra were obtained using Co radiation ( $\lambda = 1.7889 \text{ \AA}$ ) from a Bruker reflection diffractometer.

The crystal size,  $\tau$ , was determined from the broadening of the (1 0 1) reflection of anatase by Scherrer's formula:

$$\tau = \frac{K \cdot \lambda}{\beta_{\tau} \cdot \cos \theta}$$

where  $K$  is the form factor (0.9),  $\beta_{\tau}$  is the width of the peak at half the maximum intensity after subtraction of the instrumental noise, and  $\theta$  is the diffraction angle.

The absolute crystallinity of the powders for the films was determined by transmission X-ray powder diffraction using Cu K $\alpha_1$  radiation ( $\lambda = 1.5406 \text{ \AA}$ ) from a STOE Stadi P transmission diffractometer. The determination of the crystallinity of the TiO<sub>2</sub> samples is made with reference to CaF<sub>2</sub>, which is 100% crystalline. The method for determining the absolute crystallinity is described elsewhere [4].

### 2.3. DLS analysis

Dynamic light scattering (DLS) was used to measure the particle size of the different prepared TiO<sub>2</sub> powders in suspension. The samples were prepared by making a suspension containing 0.05% (w/w) TiO<sub>2</sub> in distilled water which were placed in a vial before measuring. The particle size was measured using a DLS instrument obtained from Photocor Instruments, Inc. consisting of a photon counting unit (PMT), photocorrelator, and a 633 nm 35 mW laser (JDS Uniphase).

### 2.4. DSC analysis

The Differential scanning calorimetry (DSC) investigation of the different TiO<sub>2</sub> powders samples was carried out using a Mettler Toledo DSC822e with a TSO801RO auto sampler. The samples were prepared by placing 6.0 mg TiO<sub>2</sub> powder in an aluminum container which was placed in the calorimeter. The heat transfer rate used in the investigation was 10 °C/min and the applied temperature interval was 35–550 °C.

**Table 1**  
Measured particle properties

|  | Degussa P25 | Hombikat UV100 | SC 134    | Sol-gel film |
|--|-------------|----------------|-----------|--------------|
| Crystallinity                              |             |                |           |              |
| Anatase (%)                                | 75.6        | 86.2           | 65.6      | 69.1         |
| Rutile (%)                                 | 21.6        | –              | –         | –            |
| Amorphous (%)                              | 2.8         | 13.8           | 34.4      | 30.9         |
| Crystallite size determined by XRD         |             |                |           |              |
| Crystallite size powder (nm)               | 18          | 12             | 7         | 10           |
| Crystallite size film (nm)                 | 23          | 10             | 7         | 11           |
| AFM  |             |                |           |              |
| Surface roughness (nm)                     | 59.9        | 131.7          | 198.7     | 24.4         |
| BET  |             |                |           |              |
| Surface area powder (m <sup>2</sup> /g)    | 50          | 360            | 221       | 117          |
| DLS  |             |                |           |              |
| Particle size of powder in suspension (nm) | 600 ± 15    | 818 ± 24       | 1274 ± 36 | 270 ± 2      |

### 2.5. AFM analysis

AFM analysis of the TiO<sub>2</sub> films was performed under ambient conditions using a commercial Digital Instruments Nanoscope IIIa MultiMode SPM (Veeco Instruments, Santa Barbara, CA) present at Institute of Physics, University of Aarhus. Standard V-shaped silicon tips (Ultrasharp cantilevers, NSC11, MikroMasch Germany) were used with a resonance frequency of 45 kHz, a spring constant of 1.5 N/m and a tip radius of 10.0 nm. AFM images were obtained in tapping mode at 2 Hz scan rates. The sample used in the measurement was coated onto glass.

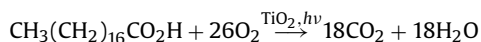
### 2.6. XPS analysis

The XPS analysis of the TiO<sub>2</sub> films before and after UV irradiation was carried out in a UHV chamber on a SX700 at the synchrotron source at the Institute for Storage Ring Facilities at Aarhus University, employing a Zeiss SX700 plane grating monochromator. The chamber was equipped with a VG CLAM2 electron spectrometer running with a pass energy of 30 eV and a slit width of 2 mm. The base pressure was around  $8 \times 10^{-10}$  mbar. The TiO<sub>2</sub> films used in the XPS analysis were cast onto stainless steel in order to prevent charging of the sample, after drying for 30 min the films were calcinated for 1 h at 450 °C. The samples were UV irradiated for 1 h outside the UHV chamber in ambient atmosphere (45% RH) using one 9 W germinal bulb (254 nm) with an aluminium reflector placed 5 cm above the samples. After UV irradiation the films were readily placed in the UHV chamber. The UV light intensity at the surface of the TiO<sub>2</sub> film was measured using a UV-meter to 30 W/m<sup>2</sup>. The obtained XPS spectra were fitted by one or more Pseudo-Voigt functions as described in [3]. The atomic concentration was determined by dividing the integrated intensities by the relative sensitivity factors, which for titanium is 1.8 and 0.66 for oxygen [3].

### 2.7. Evaluation of the photocatalytic activity

The photocatalytic activity of the prepared nanocrystalline TiO<sub>2</sub> films was investigated using stearic acid as a model compound. Previous work done by different groups has shown that the destruction of stearic acid by semiconductor photocatalysis produces no gas products other than carbon dioxide and water [12,18]. In addition it was shown that the ratio of the number of moles of stearic acid lost due to photocatalytic degradation of stearic acid to the number of moles of carbon dioxide generated is in the stoichiometric ratio of 1:18 [18].

The photocatalytic degradation of stearic acid is therefore thought to follow the reaction scheme shown below:



In order to deposit stearic acid on the TiO<sub>2</sub> film a stearic acid solution was made from 0.5 g stearic acid dissolved in 100 ml chloroform. The stearic acid solution was deposited by a pipette until the whole surface of the film was covered and then spun at 1000 rpm for 10 s using a spin coater. The samples were UV irradiated using the same 9 W germinal bulb (254 nm, UV-light intensity 30 W/m<sup>2</sup>), as for the XPS measurements.

The degradation of stearic acid was monitored by FT-IR absorbance spectroscopy, through the disappearance of the peak at 2957.5 cm<sup>-1</sup> corresponding to the asymmetric C–H stretching of the CH<sub>3</sub> group, and the peaks at 2922.8 cm<sup>-1</sup> and 2853.4 cm<sup>-1</sup> corresponding to the asymmetric and symmetric C–H stretching of the CH<sub>2</sub> group. In the present work the integrated area under these peaks (2800–3000 cm<sup>-1</sup>) was used to measure the concentration of stearic acid as a function of irradiation time. The FT-IR measurements were carried out using a FT-IR spectrometer (PerkinElmer Spectrometer, Paragon 1000).

## 3. Results and discussion

### 3.1. XRD analysis

The crystallinity of TiO<sub>2</sub> has been proposed by different research groups to influence the photocatalytic activity [4,5,19]. Normally, the crystallinity of TiO<sub>2</sub> is determined by XRD analysis from the relative intensities of the peaks corresponding to the anatase and rutile phase [4]. However, the absolute crystallinity is seldom determined, which means that the amorphous fraction of the sample is often neglected. This could have a huge impact on the interpretation of the results since it has been shown that amorphous fraction of TiO<sub>2</sub> has no or little photocatalytic activity [2].

The absolute crystallinity of the films was determined by transmission X-ray powder diffraction with reference to CaF<sub>2</sub>. The results obtained from transmission XRD show that Degussa P25 is the only sample consisting of both anatase and rutile. Degussa P25 consists of 75.6% anatase and 21.6% rutile. The remaining 2.8% may be due to an amorphous fraction of the TiO<sub>2</sub> or to the uncertainty of the method. In comparison Hombikat UV100 was found to consist of about 86.2% anatase and the SC 134 and sol-gel film of about 70% anatase. The crystallinity data are shown in Table 1. From Table 1 it is seen that the crystallite size of TiO<sub>2</sub> films determined by reflection XRD of the prepared films was in the interval 7–23 nm. The level of crystallinity was Degussa P25 > Hombikat > Sol-gel > SC 134. Fur-

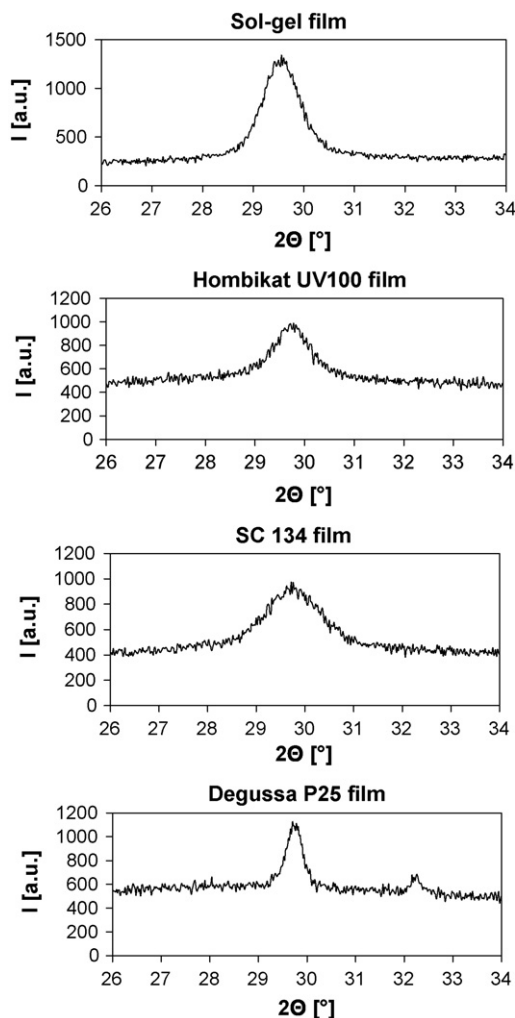


Fig. 1. XRD spectra of the prepared TiO<sub>2</sub> films.

thermore, the reflection XRD spectra of the TiO<sub>2</sub> films shown in Fig. 1 confirm that the film prepared by deposition of Degussa P25 is the only film consisting of both anatase and rutile.

### 3.2. DSC analysis

The DSC results of the TiO<sub>2</sub> powders are shown in Fig. 2. The region from 30 to 150 °C can be ascribed to desorption of physical adsorbed water and hydroxyl groups. As the powders were calcinated at 450 °C for 1 h the samples did not show evidence of the existence of residual carbon originating from the preparation method, which would have been observed as an exothermic peak in the temperature region from 200 to 350 °C [5,20,21]. From the DSC spectra it is seen that Hombikat UV100 has the greatest amount of adsorbed water on the surface followed by SC 134, sol-gel, and Degussa P25. The amount of adsorbed water or surface hydroxyl groups is suggested to be related to the specific surface area of the particles, which was confirmed by BET data shown in Table 1.

### 3.3. AFM and DLS analysis

The TiO<sub>2</sub> films were investigated using atomic force microscopy (AFM). The surface images obtained using AFM are shown in Fig. 3. From the AFM images it is seen that the TiO<sub>2</sub> film prepared from

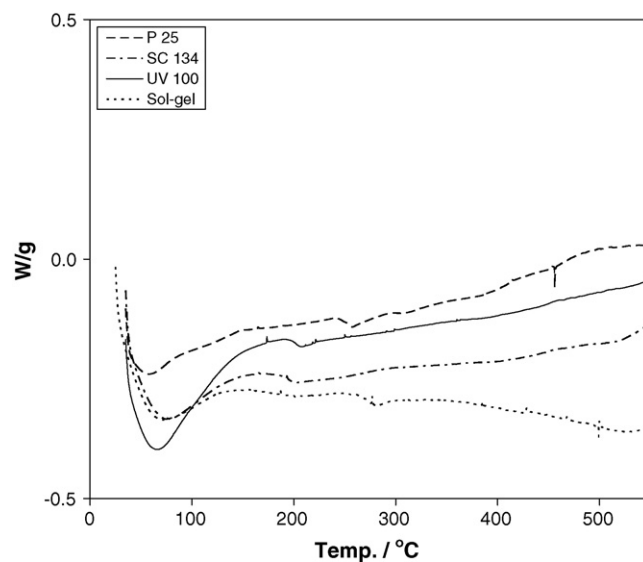


Fig. 2. DSC spectra of the Prepared TiO<sub>2</sub> films.

immobilization of SC 134 consists of larger particles or aggregates of particles compared to the other films. In comparison the sol-gel film and the film prepared from Degussa P25 are more uniform consisting of smaller aggregates. This is also seen from the roughness data presented in Table 1. DLS measurements were used to verify that the particle size of the powders in suspension can be found as the size of the particle aggregates in the films. The size of the aggregates in suspension were measured to; Sol-gel (270 nm) < Degussa P25 (600 nm) < Hombikat UV100 (818 nm) < SC 134 (1274 nm).

### 3.4. XPS analysis before and after UV irradiation

XPS is a highly sensitive technique for surface analysis which effectively can be used to investigate the composition and chemical states of the surface. In this study the surface of the prepared TiO<sub>2</sub> films were investigated before and after 1 h of UV irradiation to measure if the photo-excitation changes the surface properties of the film. In the following the peaks corresponding to Ti 2p and O 1s are analyzed.

#### 3.4.1. Analysis of the titanium 2p peak

The titanium peaks for the films are located at 458.7 eV (Ti 2p<sub>3/2</sub>) and 464.4 eV (Ti 2p<sub>1/2</sub>). The sharp and strong peak at 458.7 indicates that the Ti element mainly existed as Ti(IV) [19,22]. All the XPS spectra were very similar indicating that UV irradiation under these conditions does not induce a significant change in the Ti chemical states resulting in the formation of Ti(III) or Ti(II) that have been suggested by other groups [20,21]. Typical Ti spectra for the sol-gel film before and after UV irradiation are shown in Fig. 4.

#### 3.4.2. Analysis of the oxygen 1s peak

The XPS spectra of the O 1s peak of a typical TiO<sub>2</sub> film before and after UV irradiation are shown in Fig. 5. From the XPS spectra it is seen that the oxygen peak is asymmetric indicating that at least two different chemical states of oxygen are present. In literature the O 1s peak has been proposed to consist of 4–5 contributing species such as Ti–O in TiO<sub>2</sub> and Ti<sub>2</sub>O<sub>3</sub>, hydroxyl groups, C–O bonds, and adsorbed H<sub>2</sub>O [23]. Although some H<sub>2</sub>O is easily adsorbed on the surface of TiO<sub>2</sub> films during the deposition process the physically adsorbed H<sub>2</sub>O on TiO<sub>2</sub> is easily desorbed under the ultrahigh vacuum condition of the XPS system. Only negligible amounts of physisorbed water remains on the surface of the TiO<sub>2</sub> films. Hence,



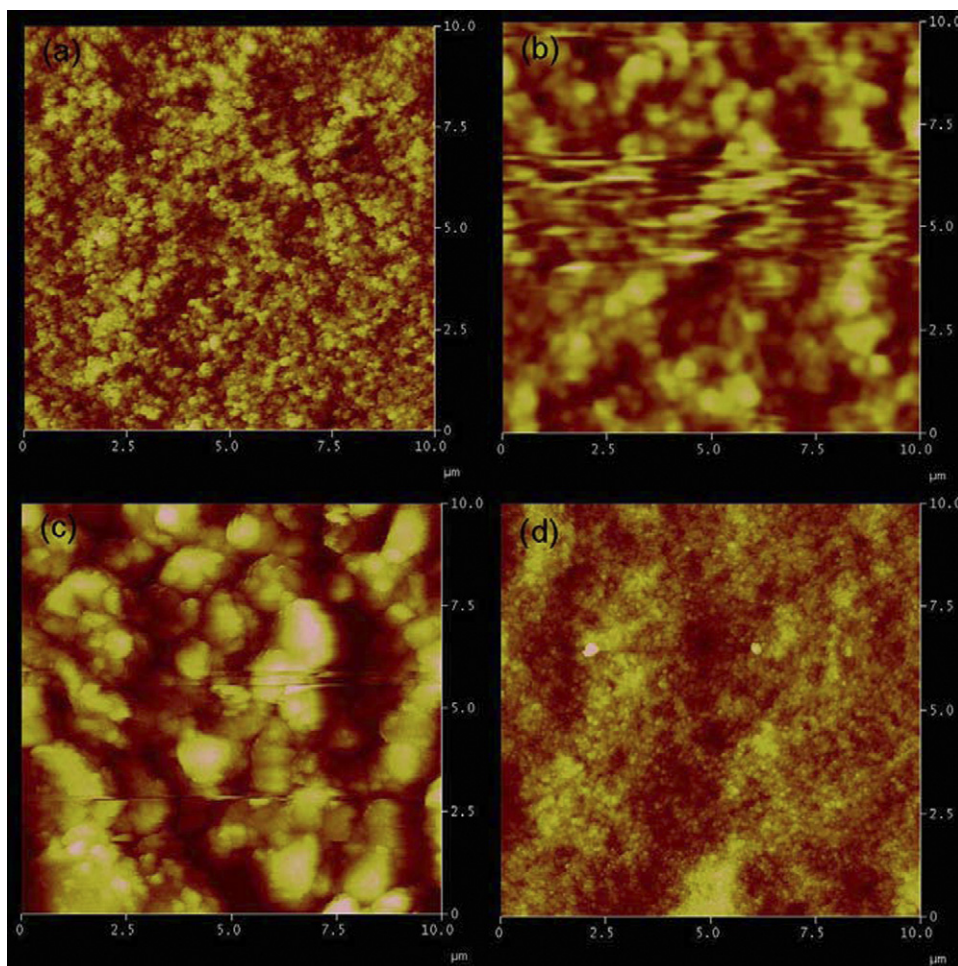


Fig. 3. AFM images of the surface of (a) the Degussa P25 film, (b) the Hombikat UV100 film, (c) the SC 134 film, and (d) the sol-gel film.

the hydroxyl on the surface can be attributed to Ti–OH on the films [15]. The peaks located at 529.9 and 531.9 eV therefore can be assumed to correspond to Ti–O in TiO<sub>2</sub> and hydroxyl groups (–OH), respectively [24]. In this work the O 1s peak is modeled with two Pseudo-Voigt functions corresponding to surface oxygen (1) and lattice oxygen (2), respectively [3].

From the O 1s spectrum of the sol-gel film before UV irradiation it is seen that most of the oxygen is present as lattice oxygen. In comparison the XPS spectrum after 1 h of UV irradiation shows a significant change in the amount of surface oxygen. After UV illumination the relative area of the peak due to surface oxygen (hydroxyl groups) increases significantly indicating that chemisorption of

water molecules on the surface of the TiO<sub>2</sub> films is enhanced by UV irradiation. Usually, an increase in the hydroxyl content on the surface of TiO<sub>2</sub> films enhances both the photo-induced superhydrophilicity and photocatalytic activity [24]. The modeled peak data is shown in Table 2 for all four TiO<sub>2</sub> films.

The peak data in Table 2 shows that about 26% of the oxygen is present in a form of surface oxygen (hydroxyl groups) prior to UV irradiation. The difference in surface oxygen between the films can be ascribed to the difference in surface roughness and surface areas [6]. The films prepared from the smallest particles or aggregates (DLS measurements) in this case the sol-gel film can be assumed to have the largest surface area.

**Table 2**

Fitted parameters for the O 1s peak of the TiO<sub>2</sub> films before and after UV irradiation

|   | Degussa P25 | Hombikat UV100 | SC 134 | Sol-gel film |
|---|-------------|----------------|--------|--------------|
| <b>O 1s peak data</b>                   |             |                |        |              |
| Area <sub>surface</sub> (%)             | 28.0        | 25.7           | 24.0   | 28.8         |
| Area <sub>lattice</sub> (%)             | 72.0        | 74.3           | 76.0   | 71.2         |
| E <sub>b</sub> (eV) Ti–O                | 529.9       | 529.9          | 529.9  | 529.9        |
| E <sub>b</sub> (eV) OH                  | 531.8       | 531.9          | 531.8  | 531.8        |
| <b>O 1s peak data after UV</b>          |             |                |        |              |
| Area <sub>surface</sub> (%)             | 34.4        | 34.0           | 30.1   | 35.8         |
| Area <sub>lattice</sub> (%)             | 65.6        | 66.0           | 68.9   | 64.2         |
| E <sub>b</sub> (eV) Ti–O                | 529.9       | 529.9          | 529.9  | 529.9        |
| E <sub>b</sub> (eV) OH                  | 531.9       | 531.7          | 531.9  | 531.9        |
| Relative increase in surface oxygen (%) | 23.9        | 32.1           | 25.4   | 24.5         |

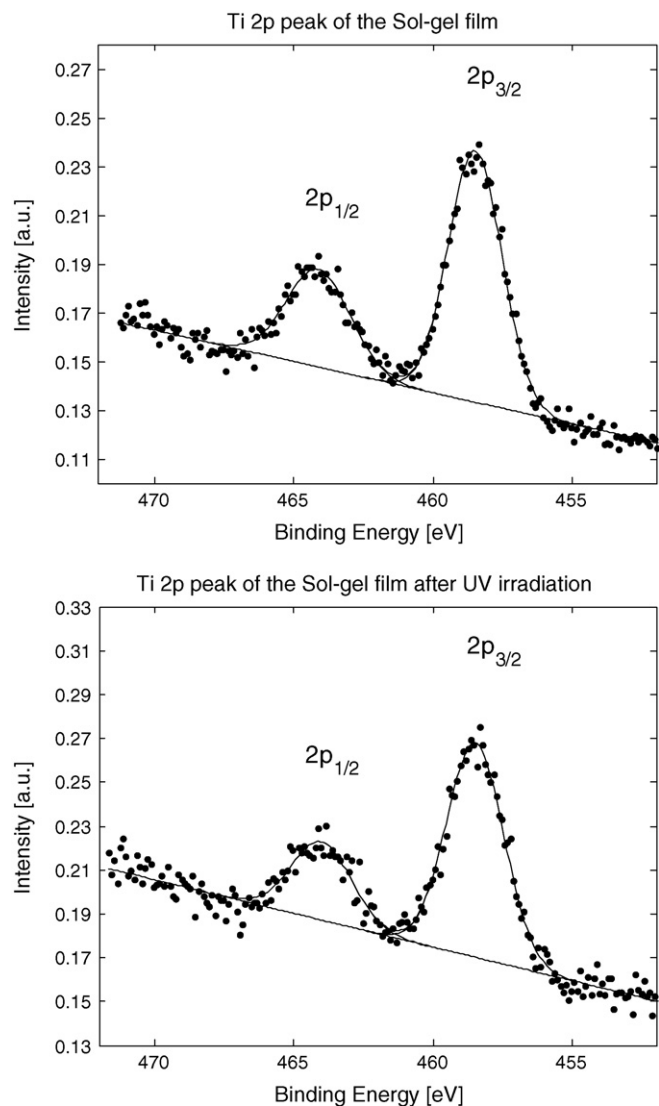


Fig. 4. XPS spectrum of the Ti 2p peak of the sol-gel film before and after 1 h of UV irradiation.

After 1 h of UV irradiation the percentage of surface oxygen is increased by up to 32% of the amount prior to UV irradiation. In order to compare the amount of oxygen which is present as surface oxygen in the different  $\text{TiO}_2$  films before and after 1 h of UV irradiation the atomic ratio between the crystal lattice oxygen and Ti was studied by area determination and known cross sections for the interaction between atoms and X-rays. The calculated ratios are presented in Table 3.

**Table 3**  
Oxygen content and oxygen to titanium ratios

|   | Atomic ratio of $\text{O}_{\text{lattice}}\text{-Ti}$ | Atomic ratio of $\text{O}_{\text{total}}\text{-Ti}$ |
|---|---|---|
| <b><math>\text{TiO}_2</math> films</b>                      |   |   |
| Degussa P25 film  | 2.00  | 2.64  |
| Hombikat UV100 film   | 1.82  | 2.45  |
| SC 134 film   | 1.82  | 2.52  |
| Sol-gel film  | 1.87  | 2.62  |
| <b><math>\text{TiO}_2</math> films after UV irradiation</b> |   |   |
| Degussa P25 film  | 1.88  | 2.87  |
| Hombikat UV100 film   | 1.82  | 2.76  |
| SC 134 film   | 1.96  | 2.85  |
| Sol-gel film  | 1.91  | 2.97  |

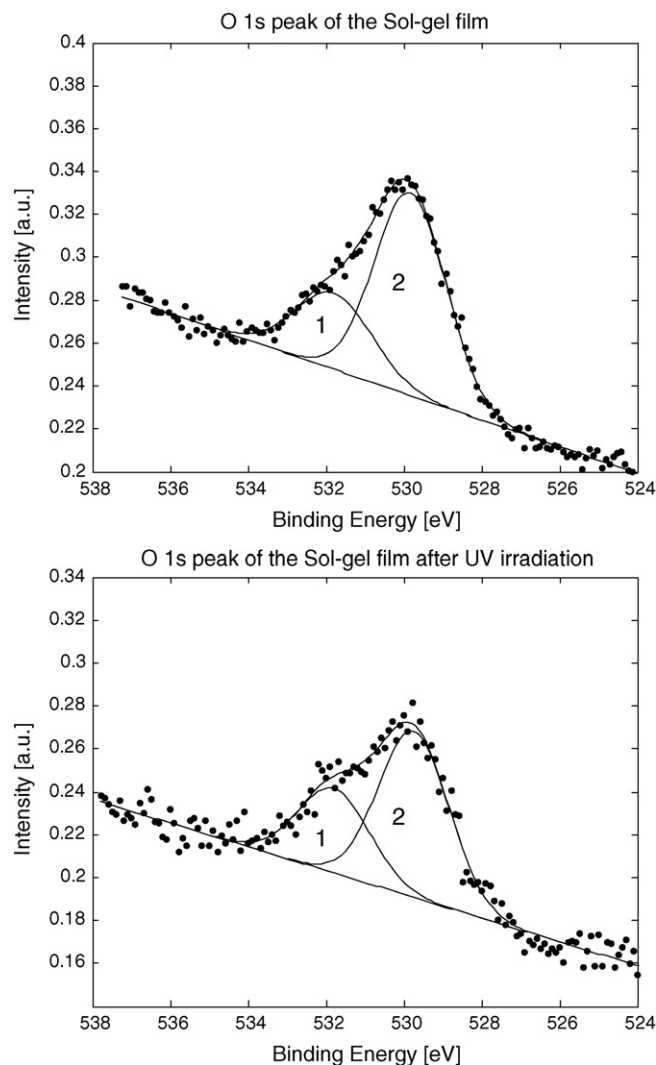


Fig. 5. XPS spectra of the O 1s peak of the sol-gel film before and after UV irradiation. Peak 1 is due to surface oxygen probably due to OH groups and peak 2 is due to lattice oxygen in the form of Ti–O–Ti bonds.

From Table 3 it is seen that the atomic ratio between crystal lattice oxygen and Ti were found to be around 1.9 both before and after UV irradiation. Without a standard  $\text{TiO}_2$  reference surface, it is not possible to use these ratios quantitatively, the ratios is therefore only used semi-quantitatively to obtain knowledge about changes in surface and lattice oxygen.

Comparison of the ratios between total oxygen and Titanium show that the ratio before and after UV irradiation vary significantly. After UV illumination the total oxygen/Ti ratio has increased indicating an increase in the oxygen present at the surface most likely as chemisorbed hydroxyl groups.

The increase in hydroxyl groups after UV irradiation supports the idea that UV irradiation promotes the generation of reactive species that will mediate the photocatalytical destruction of pollutants. These results are similar to the results reported by Yu et al. who also observed an increase in the hydroxyl group content after UV irradiation using high resolution XPS analysis [24].

STM investigations of rutile (110)  $\text{TiO}_2$  single crystals have shown that a significant amount of oxygen vacancies are present on the surface of single crystals [25]. Besenbacher and co-workers has conducted a detailed study of the interaction of oxygen and water with the vacancies on the single crystals [25]. The investigation

showed that after interaction between dioxygen and the vacancies lattice oxygen was observed where originally a vacancy was located and a second oxygen atom was found in a five-coordinated position on top of a titanium atom indicating that a splitting of the dioxygen molecule has occurred. Interaction between water and the vacancies resulted in chemisorbed hydroxyl groups located in the original vacancy position. A second hydroxyl group was found very close to this indicating a transfer of a proton from the chemisorbed water molecule to a neighboring bridging oxygen.

Our group believes that the increase in the amount of hydroxyl groups observed by the XPS investigation in the present work after UV irradiation has two origins. First existing oxygen vacancies in the  $\text{TiO}_2$  films were occupied by water molecules after pretreatment of the films. Water is adsorbed easily on the  $\text{TiO}_2$  films and occupies the vacancies even if it is present in almost negligible amounts [25]. Interaction between the vacancy and the water molecule has lead to diffusion of a proton to a neighbor oxygen atom thereby creating two hydroxyl groups. According to the DFT calculation conducted by Besenbacher and co-workers the system is stabilized by diffusion of a proton to a more distant oxygen atom [25]. The diffusion to distant oxygen atoms is catalyzed by the presence of water molecules [26]. Adsorption of dioxygen can stabilize the system even further by splitting the dioxygen molecule thereby occupying a vacancy [25]. However, this process is not believed to occur to a greater extent if the principle part of the vacancies is already occupied by hydroxyl groups. That dioxygen did not occupy these vacancies immediately after creation is a result of the difference in kinetics between the two competing molecules (dioxygen and water) during interaction with the oxygen vacancies. Secondly, an increased amount of oxygen vacancies are induced by the UV irradiation. These vacancies are yet again believed to be occupied by water molecules resulting in diffusion of a proton to a neighboring oxygen atom as described above, thereby increasing the amount of hydroxyl groups on the surface.

According to DFT calculations of the species found on rutile [25] it can be calculated that it requires 3.25 eV to create an oxygen vacancy on rutile. If we compare the stability of a rutile crystal to an anatase crystal the bonding energy of an oxygen atom on the surface of anatase is believed to be even smaller than 3.25 eV due to the lower density of the anatase crystal. This energy corresponds to a wavelength of 382 nm. Thus, the UV C light (253.7 nm) used in our

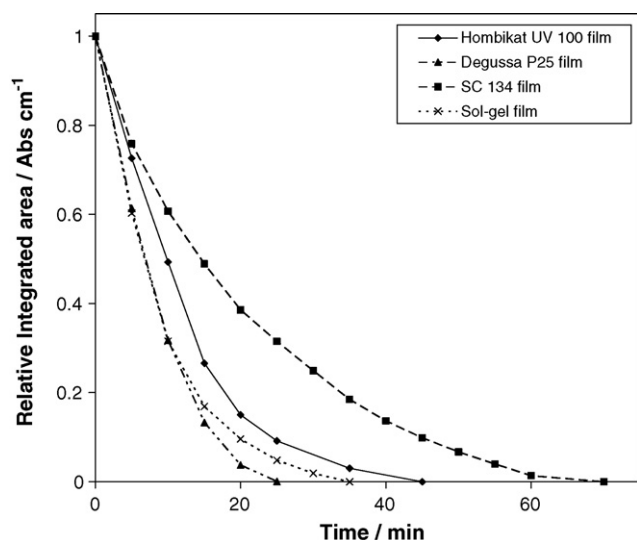


**Fig. 6.** The degradation of stearic acid on the  $\text{TiO}_2$  films. The measured activity of the  $\text{TiO}_2$  films is; Degussa P25 > Sol-gel > Hombikat UV100 > SC 134. Relative integrated area of 1 corresponds to  $6.5 \text{ Abs cm}^{-1}$ .

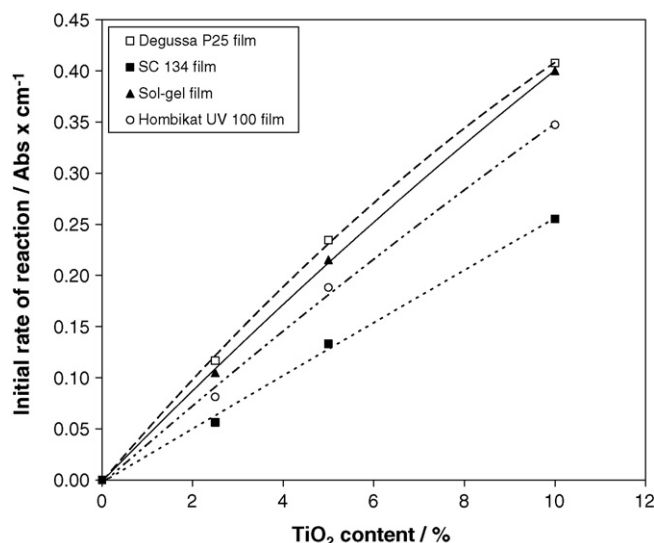


**Fig. 7.** Initial rate of degradation of stearic acid on the  $\text{TiO}_2$  films as a function of the  $\text{TiO}_2$  content in the films.

experiments has sufficient energy to create extra oxygen vacancies [7].

In the photocatalytic process the hydroxyl groups on the surface are active in the oxidation process of adsorbed organics by capturing a hole ( $h^+$ ) from the excited crystal resulting in formation for hydroxyl radicals. Usually, an increase in the hydroxyl content on the surface of  $\text{TiO}_2$  films enhances both the photocatalytic activity and the superhydrophilicity [24]. Currently, the investigation of the mechanism involved in the photo-induced superhydrophilicity is carried out.

If the  $\text{TiO}_2$  films are stored in the dark, the surface of the  $\text{TiO}_2$  film will convert back to its initial more hydrophobic state. The regeneration of the hydrophobic surface in the dark is thought to be caused by either adsorption of organics or by release of water due to adsorption of dioxygen creating a more hydrophobic surface [7,27,28]. However, hydroxyl groups will still be present on the  $\text{TiO}_2$  surface.

In this work about the same increase in the amount of hydroxyl groups was observed independent of which powder or method was used to prepare the  $\text{TiO}_2$  films. In addition the absolute amount of hydroxyl groups varied a little between the films. However, a correlation between the amount of hydroxyl groups and the photocatalytic activity was found (see below).

### 3.5. Determination of the photocatalytic activity

The photocatalytic activity of the prepared  $\text{TiO}_2$  films was investigated from the degradation profiles of stearic acid. Fig. 6 shows the degradation of stearic acid on the four  $\text{TiO}_2$  films. The measured activity of the  $\text{TiO}_2$  films by degradation of stearic acid is; Degussa P25 > Sol-gel > Hombikat UV100 > SC 134.

In order to compare the activity of the different films quantitatively the initial rate of degradation of stearic acid was used. Fig. 7 shows that the rate of degradation increases nearly linear with the concentration of  $\text{TiO}_2$  in the films. These findings suggest that the amount of  $\text{TiO}_2$  in the film is the limiting condition for the rate of reaction. The observed increase in the rate of degradation is probably due to an increased absorption of UV light due to larger amount of crystalline material. From Fig. 7 it is seen that the film prepared from Degussa P25 is the most active film, followed by the sol-gel film, Hombikat UV100 film, and the SC 134 film.



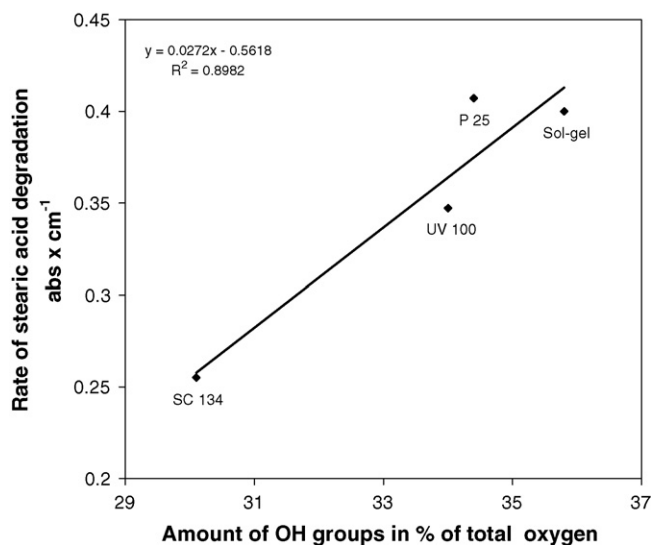


Fig. 8. Photocatalytic activity of the TiO<sub>2</sub> film as a function of the amount of surface OH groups determined by XPS investigation after UV irradiation.

In Fig. 8 the activity of the TiO<sub>2</sub> is plotted against the amount of surface OH groups determined by XPS investigation after UV irradiation. The resulting plot shows that there is a good correlation between the amount of OH groups on the surface and the photocatalytic activity.

The activity of the films is believed to be related to the crystallinity of the TiO<sub>2</sub> film and the amount of surface area and surface hydroxyl groups. The crystallinity data determined by XRD shown in Table 1 confirms this idea. The Degussa P25 film was the only film consisting of both anatase and rutile. The anatase/rutile structure of titania has been suggested by different research group to be beneficial for suppressing the recombination of photogenerated electrons and holes and thus enhance the photocatalytic activity [29,30]. The crystallinity of the film prepared from Hombikat UV100 was found to consist of 86.2% anatase. In comparison the sol-gel film and the SC 134 film were both found to consist of about 70% anatase. Additionally, the particle size of the TiO<sub>2</sub> powders used in suspension to prepare the films is believed heavily to influence the activity and stability of the films. In this work it was found that the particles or aggregates in suspension used in the preparation of the different films varied from 270 to 1274 nm in diameter depending on the preparation method of the TiO<sub>2</sub> powders (Table 1). It was found that the sol-gel prepared TiO<sub>2</sub> and Degussa P25 had the smallest particle size, which resulted in these powders, produced the most uniform and homogeneous films having the lowest surface roughness measured by AFM. Based on AFM imaging the Sol-gel and Degussa P25 films have the largest surface area available for reaction as they are assembled from smaller particles. Moreover, the results obtained from XPS analysis of the surfaces after UV irradiation showed that the sol-gel film and the Degussa P25 film had the highest amount of adsorbed hydroxyl groups consisting with these films have the largest surface area.

#### 4. Conclusion

The investigation of the different prepared TiO<sub>2</sub> films showed that the film prepared from Degussa P25 and the sol-gel film were the most active films, followed by the Hombikat UV100 film and the SC 134 film. The activity of the films is assumed to be related to the crystallinity of the TiO<sub>2</sub> film and the amount of surface area and surface hydroxyl groups.

Based on the XPS investigation of the films before and after UV irradiation it was suggested that the photocatalytic destruction of organic matter on TiO<sub>2</sub> films proceeds partly through formation of hydroxyl radicals which are formed from adsorbed hydroxyl groups. The increase in hydroxyl groups observed by XPS analysis of the surface of the TiO<sub>2</sub> films is believed to originate from adsorption of water in the vacancies. Interaction between water and the vacancy is thought to promote diffusion of a proton to a neighboring oxygen, thereby increasing the amount of hydroxyl groups on the surface. Furthermore a good correlation between the amount of OH groups on the surface of the different TiO<sub>2</sub> films and the photocatalytic activity was found.

The sol-gel synthesized TiO<sub>2</sub> and the Degussa P25 had the smallest particle size, which resulted in these powders, produced the most uniform and homogeneous films having the lowest surface roughness measured by AFM. Based on AFM imaging of the Sol-gel and the Degussa P25 film and the particle size these films have the largest surface area available for reaction. Moreover, the results obtained from XPS analysis of the surfaces after UV irradiation showed that the sol-gel film and the Degussa P25 film had the highest amount of adsorbed hydroxyl groups consisting with these films have the largest surface area.

The investigation also showed that the rate of degradation increases nearly linearly with the concentration of TiO<sub>2</sub> in the solvents used in preparation of the films. These findings suggest that the amount of TiO<sub>2</sub> in the films is the limiting condition for the rate of reaction. The observed increase in the rate of degradation is probably due to an increased absorption of UV light due to larger amount of crystalline material.

#### Acknowledgements

We would like to thank Chemical Institute University of Aarhus for their help with the conduction of the XRD analysis of the titania films and the use of equipment. We would also like to thank Ph.D. student Dong Mingdong Department of Physics and Astronomy University of Aarhus for his help with the AFM analysis of the films.

#### References

- [1] A.L. Linsebigler, G. Lu, J.T. Yates Jr., *Chem. Rev.* 95 (1995) 735–758.
- [2] A. Mills, S. Le Hunte, *J. Photochem. Photobiol. A* 108 (1997) 1–35.
- [3] H. Jensen, A. Soloviev, Z. Li, E.G. Søgaard, *Appl. Surf. Sci.* 246 (2005) 239–249.
- [4] H. Jensen, K.D. Joensen, J.-E. Jørgensen, J.S. Pedersen, E.G. Søgaard, *J. Nanopart. Res.* 6 (2004) 519–526.
- [5] M. Kang, S.-Y. Lee, C.-H. Chung, S.M. Cho, G.Y. Han, B.-W. Kim, K.J. Yoon, *J. Photochem. Photobiol. A* 144 (2001) 185–191.
- [6] J. Yu, J. Xiong, B. Cheng, S. Liu, *Appl. Catal. B: Environ.* 60 (2005) 211–221.
- [7] O. Carp, C.L. Huisman, A. Reller, *Prog. Solid State Chem.* 32 (2004) 33–177.
- [8] A. Mills, S.-K. Lee, *J. Photochem. Photobiol. A: Chem.* 152 (2002) 233–247.
- [9] A. Fujishima, X. Zhang, C. R. Chimie 9 (2006) 750–760.
- [10] P.S. Mukherjee, A.K. Ray, *Chem. Eng. Technol.* 22 (3) (1999) 253–260.
- [11] T.E. Doll, F.H. Frimmel, *Acta Hydrochim. Hydrobiol.* 32 (3) (2004) 201–213.
- [12] A. Mills, G. Hill, S. Bhopal, I.P. Parkin, S.A. O'Neill, *J. Photochem. Photobiol. A* 160 (2003) 185–194.
- [13] H. Jensen, J.H. Pedersen, J.E. Jørgensen, J.S. Pedersen, K.D. Joensen, S.B. Iversen, E.G. Søgaard, *J. Exp. Nanosci.* 1 (3) (2006) 355–373.
- [14] H. Jensen, K.D. Joensen, S.B. Iversen, E.G. Søgaard, *Ind. Eng. Chem. Res.* 45 (10) (2006) 3348–3353.
- [15] J.-G. Yu, H.-G. Yu, B. Cheng, X.-J. Zhao, J. Yu, W.-K. Ho, *J. Phys. Chem. B* 107 (2003) 13871–13879.
- [16] A. Mills, N. Elliott, G. Hill, D. Fallis, J.R. Durrant, R.L. Willis, *J. Photochem. Photobiol. Sci.* 2 (2003) 591–596.
- [17] C.J. Barbé, F. Arendse, P. Comte, M. Jirousek, F. Lenzmann, *J. Am. Ceram. Soc.* 80 (12) (1997) 3157–3171.
- [18] T. Minabe, D.A. Tryk, P. Sawunyama, Y. Kikuchi, K. Hashimoto, A. Fujishima, *J. Photochem. Photobiol. A* 137 (2000) 53–62.
- [19] H. Liu, W. Yang, Y. Ma, Y. Cao, J. Yao, J. Zhang, T. Hu, *Langmuir* 19 (2003) 3001–3005.
- [20] J. Yu, X. Zhao, Q. Zhao, *Thin Solid Films* 379 (2000) 7–14.

- [21] J. Liqiang, S. Xiaojun, C. Weimin, X. Zili, D. Yaogou, F. Honggang, J. Phys. Chem. Solids 64 (2003) 615–623.
- [22] W. Que, Y. Zhou, Y.L. Lam, Y.C. Chan, C.H. Kam, Appl. Phys. A 73 (2001) 171–176.
- [23] Y. Naganuma, S. Tanaka, C. Kato, Jpn. J. Appl. Phys. 43 (9A) (2004) 6315–6318.
- [24] J. Yu, J.C. YU, W. Ho, Z. Jiang, New J. Chem. 26 (2002) 607–613.
- [25] S. Wendt, R. Schaub, J. Matthiesen, E.K. Vestergaard, E. Wahlström, M.D. Rasmussen, P. Thstrup, L.M. Molina, E. Lægsgaard, I. Stensgaard, B. Hammer, F. Besenbacher, Surf. Sci. 598 (2005) 226–245.
- [26] S. Wendt, J. Matthiesen, R. Schaub, E.K. Vestergaard, E. Lægsgaard, F. Besenbacher, B. Hammer, Phys. Rev. Lett. 96 (2006) 066107.
- [27] A. Mills, M. Crow, J. Phys. Chem. C 111 (2007) 6009–6016.
- [28] K. Hashimoto, H. Irie, A. Fujishima, Jpn. J. Appl. Phys. 44 (12) (2005) 8269–8285.
- [29] R.I. Bickley, T. Gonzalez-Carreno, J.S. Lees, L. Palmisano, R.J.D. Tilley, J. Solid State Chem. 92 (1991) 178–190.
- [30] J. Yu, J.C. Yu, M.K.-P. Leung, W. Ho, B. Cheng, X. Zhao, J. Zhao, J. Catal. 217 (2003) 69–78.